Plasma Chem Plasma Process (2010) 30:553–563
DOI 10.1007/s11090-010-9237-4

ORIGINAL PAPER

Effects of Oxygen Addition and Treating Distance on Surface Cleaning of ITO Glass by a Non-Equilibrium Nitrogen Atmospheric-Pressure Plasma Jet

M.-H. Chiang · K.-C. Liao · I.-M. Lin · C.-C. Lu · H.-Y. Huang · C.-L. Kuo · J.-S. Wu · C.-C. Hsu · S.-H. Chen

Received: 26 March 2010 / Accepted: 1 June 2010 / Published online: 15 June 2010

Abstract Effects of oxygen addition and treating distance on cleaning organic contaminants on stationary and non-stationary (1–9 cm/s) ITO glass surfaces by a parallel-plate nitrogen-based dielectric barrier discharge (DBD) are investigated experimentally; the DBD is driven by a 60 kHz bipolar quasi-pulsed power source. The results show that two regimes of favorable operating condition for improving the hydrophilic property of the surface (reducing the contact angle from 84° to 25–30°) are found. The measured spatial distribution of NO-γ UV emission, O_3 concentration and OES spectra are shown to strongly correlate with the measured hydrophilic property. At the near jet downstream locations ($z < 10$ mm), the metastable $N_2(A^3\sum_u^+)$ and photo-induced dissociation of ozone play dominant roles in cleaning the ITO glass surface; while at the far jet downstream locations ($z > 10$ mm), where the ratio of oxygen to nitrogen is lower, only the long-lived metastable $N_2(A^3\sum_u^+)$ plays a major role in cleaning the ITO glass surface.

Keywords Atmospheric-pressure plasma jet · DBD · ITO · Quasi-pulsed · Surface cleaning

M.-H. Chiang · I.-M. Lin · C.-C. Lu · H.-Y. Huang · C.-L. Kuo · J.-S. Wu (✉)
Department of Mechanical Engineering, National Chiao Tung University, Hsinchu 30010, Taiwan
e-mail: chongsin@faculty.nctu.edu.tw

K.-C. Liao
Department of Bio-Industrial Mechatronics Engineering, National Taiwan University, Taipei 10617, Taiwan

C.-C. Hsu
Department of Chemical Engineering, National Taiwan University, Taipei 10617, Taiwan

S.-H. Chen
Physics Division, Institute of Nuclear Energy Research, Longtan 32546, Taiwan

Introduction

Recently, atmospheric-pressure (AP) plasmas have attracted great attention [1–3], mainly because of their distinct advantages compared to low-pressure plasmas. These advantages include: 1) their relatively low cost since, there is no need to use expensive vacuum equipment; and 2) the possibility for large-scale continuous in-line processing. Thus, a thorough understanding of all aspects of AP plasmas is of critical importance, in terms of both their fundamental physics and their practical applications.

One of the major disadvantages of AP plasma is the small distance between two electrodes (order of mm) [4–6], which makes their application difficult and inflexible, although it has been shown that thin foil can still be used directly in the discharge region [7]. Thus, the use of the post-discharge jet region of atmospheric-pressure plasma may possibly remove this difficulty, although the corresponding plasma is expected to be much weaker than that in the discharge, or even to entirely disappear. However, use of the post-discharge region can render the plasma source as a stand-alone module, which could be very useful in practical applications [8, 9]. In addition, the parallel-plate type discharge, although representing the simplest geometrical configuration, has the potential for applications that require large-area uniformity. In atmospheric-pressure applications, rare gases, such as helium and argon, have generally been used [10, 11], dramatically increasing operating costs. Thus, efficient use of cheaper gases, such as nitrogen or air, has become an important issue in practical applications. Recently, Iwasaki et al. [12, 13] have shown that the post-discharge region of a remote pulse nitrogen DBD added with $\sim$0–0.2% of oxygen can be used for the surface cleaning of mobile ITO glass surfaces, and also that it can dramatically increase the corresponding hydrophilic property. A kinetic mechanism was proposed to elucidate the cleaning process of the nitrogen AP jet through the measured concentrations of reactive species, which included reactive nitrogen species (NO) and reactive oxygen species (O, O_3), by the use of optical diagnostics. Note that in their study, neither a detailed description of the pulsed power supply (e.g. voltage waveform and discharge current) nor the quality of the discharge gases was provided. In addition, thus far, no other study has systematically verified the results or investigated the effect of treating distance (between the exit of the DBD and the surface to be cleaned), both of which are important in practical applications. Thus, the major goal of this paper was to elucidate the role of oxygen addition and treating distance together in the surface cleaning of an ITO glass surface by a nitrogen-based AP plasma jet.

In the present study, we developed a parallel-plate nitrogen DBD operating under the atmospheric-pressure condition and driven by a high-voltage bipolar quasi-pulsed power supply (60 kHz). The nitrogen DBDs without, and with, the addition of traced oxygen were then applied to clean stationary, and non-stationary, ITO glass using the post-discharge jet region at different treating distances. Measurements of concentrations of several reactive species at various spatial locations under different levels of oxygen addition to nitrogen were then used to elucidate the cleaning process.

Experimental Methods

The current AP plasma consisted of two parallel copper electrodes (50 × 50 × 8 mm each) with an embedded cooling water system (see Fig. 1). Each of the electrodes was covered with a 70 × 70 × 1 mm quartz plate. The distance between the two quartz plates was fixed at 1 mm throughout the study. This DBD assembly was powered by a quasi-

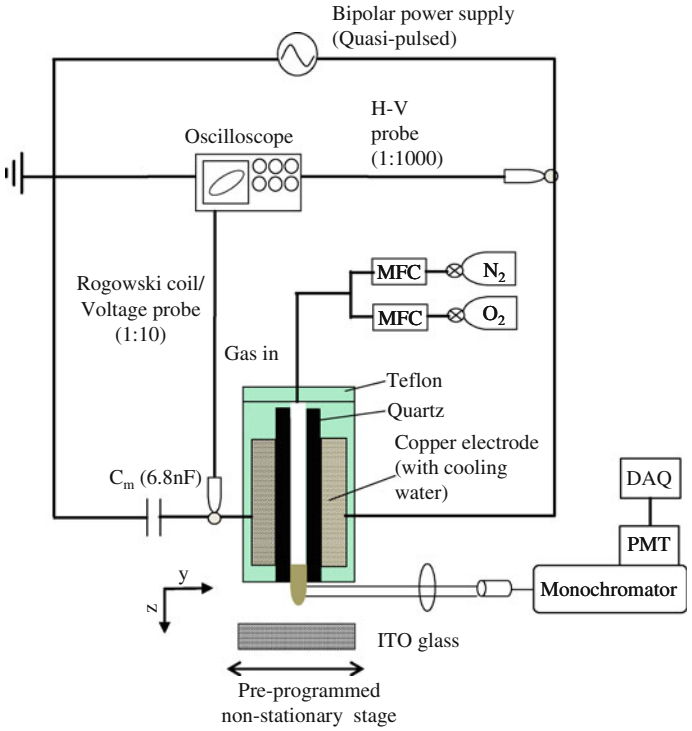

Fig. 1 Schematic sketch of a planar DBD APPJ

pulsed bipolar power supply (Model Genius-2, EN technologies Inc.) at frequencies of 20–60 kHz. Input voltage and output current waveform across the electrodes of the parallel-plate discharge were measured by a high-voltage probe (Tektronix P6015A) and a Rogowski coil (IPC CM-100-MG, Ion Physics Corporation Inc.), respectively, through a digital oscilloscope (Tektronix TDS1012B). The measured applied voltage and discharge current as a function of time are shown in Fig. 2, in which the pulse width is about 3 μs and the discharge current shows a typical filamentary type of DBD. Plasma power absorption was measured by the technique of "Lissajous figure" (Q–V characteristics) [14] using a capacitor with a capacitance of $C_m = 6.8$ nF and a voltage probe (Tektronix P2220). Discharge gas, which included pure nitrogen (99.99%), and mixtures of gases with 0.004–1% of oxygen in nitrogen, flowed from the top to the bottom between the parallel plates. The flow rates were controlled by manually adjustable flowmeters. The spectral optical emission intensities of the APPJ were measured using a monochromator (PI Acton SP 2500) with a Photomultiplier tube (Hamamatsu R928), which was mounted on a mobile 3-D table. The concentrations of O_3 were measured using an ozone monitor (API Model 450). The surface chemical composition of the ITO glass before and after application of the AP plasma jet was measured using an X-ray photoelectron spectrometer (PHI Quantera SXM, Scanning Monochromated Aluminum anode, chamber pressure below 5×10^{-10} torr). The AFM images for measuring the roughness of the sample surface were obtained using a Veeco Dimension 5000 Scanning Probe Microscope (D5000). For the clarity of presentation, all of the results presented in this paper were performed under the conditions of 60 kHz (power supply), 50 SLM (flow rate) and 175 W (plasma absorbed

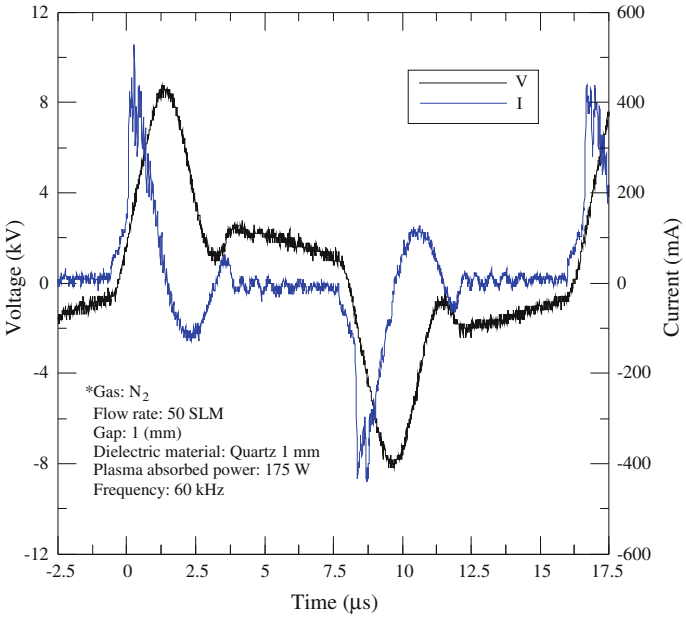

Fig. 2 Typical pulsed voltage waveform and discharge current

power). In addition, the gas temperatures (measured by K-type thermocouple) in the jet region ($z = 2$–20 mm) were generally low, in the range of 50–80°C under the typical operating condition, which was safe for ITO glass cleaning and other applications.

For the surface treatment of ITO glass, the distance between the bottom edge of the planar DBD and the ITO glass was varied in the range of $z = 2$–20 mm. Note that "z" denotes the coordinate in the downstream direction measured from the bottom edge of the DBD assembly. The ITO glass was either stationary or transported by a pre-programmed non-stationary stage. The data on the contact angle for the stationary case presented here were obtained after 5 s of plasma jet stream impinging onto a stationary ITO glass. The non-stationary speed of the ITO glass passing the DBD jet was in the range of 1–9 cm/s. The hydrophilic property (contact angle) of the glass surface was then measured using a contact angle machine (KRŰSS GH100) with a 2 μL drop of de-ionized water placed on the glass surface using a micropipette.

Results and Discussion

Figure 3 shows the measured contact angle (CA) of the stationary ITO glass surface after the plasma jet treatment, as a function of both the downstream distance and the ratio of O_2–N_2 (%). The contact angle before plasma treatment was 84°. The results show that there existed two distinct regimes with lower CAs in the range of 20–30°. The first one was the regime with an oxygen addition of less than 0.05% and a treating distance in the range of 6–16 mm. The second one was the regime with an oxygen addition larger than 0.06% and a treating distance in the range of 2–10 mm. Measured CAs in both regimes were less than 30° in general; for some conditions in the first regime, they were well below 25°,

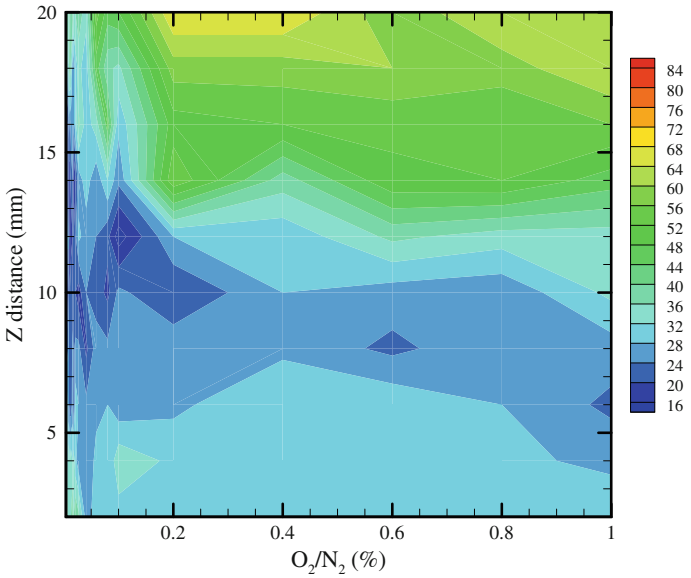

Fig. 3 Measured contact angle of ITO glass surface (stationary) as functions of z coordinate and O_2/N_2 (%) after 5 s of plasma jet treatment (60 kHz, 50 SLM, 175 W)

Table 1 Chemical composition of the ITO glass after planar-DBD APPJ treatment

O_2/N_2 (%)	z (mm)	Speed (cm/s)	Exposure time (s)	Contact angle (°)	C (%)	N (%)	O (%)	In (%)	Sn (%)	O/C
0	4	0	5	37	30.29	5.04	42.47	20.09	2.11	1.4
0	10	0	5	20	17.47	0.89	51.69	27.05	2.90	2.96
0.06	4	0	5	29	18.83	1.18	49.55	27.18	3.26	2.63
0.06	10	0	5	22	17.38	0.74	51.29	27.65	2.93	2.95
Untreated ITO				84	33.83	0.63	39.38	23.50	2.66	1.16

demonstrating that this post-discharge jet region could be used to effectively improve the hydrophilic property of ITO glass by adding trace amounts of oxygen. Table 1 summarizes the measured chemical composition of the ITO glass surface using XPS analysis and the measured CAs after plasma jet treatment. Clearly, the O/C ratio increased dramatically from 1.16 (untreated) to 2.95–2.96 ($z = 10$ mm for pure nitrogen and 0.06% oxygen cases), which was similar to the result in [15]. This meant that some carbon atoms were effectively removed by the plasma jet, which can be explained by considering the measured concentrations of O_3, UV emission (e.g., 236.6 nm, NO-γ) and other OES spectra in the jet region, which are described next.

Figure 4a, b show the measured contact angles (CA) of the ITO glass surface after pure N_2 and 0.04% O_2/N_2 plasma jet treatment for the non-stationary case (1–9 cm/s) as a function of downstream distance, respectively. The measured contact angle generally increased with increased non-stationary speed at the fixed downstream distance from the jet exit, which meant that the hydrophilic property deteriorated because of the reduced effective treatment time. However, the range of smaller contact angles for the 0.04% O_2/N_2

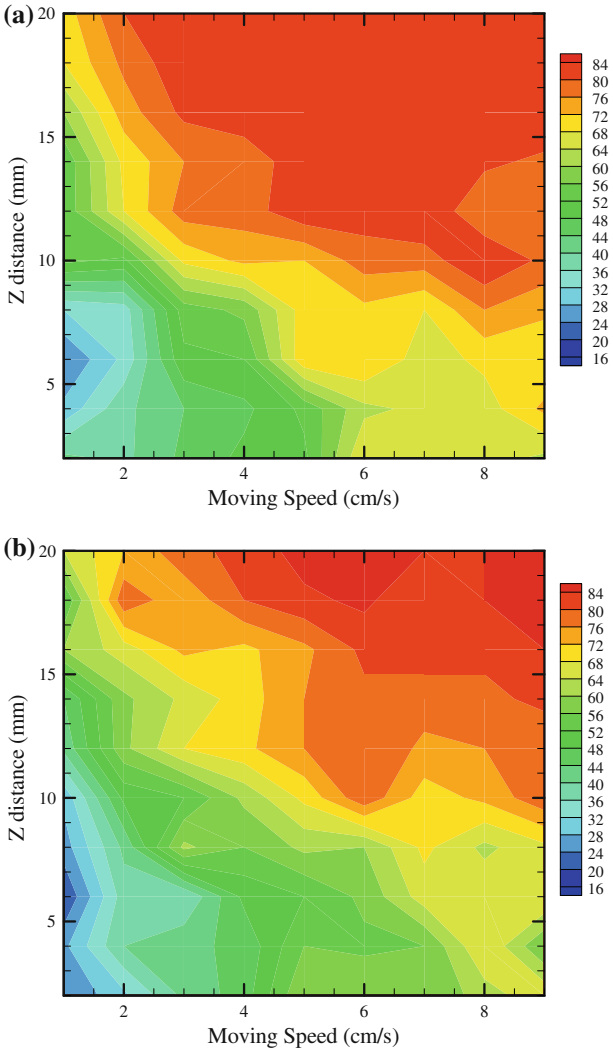

Fig. 4 Measured contact angle of ITO glass surface (non-stationary) as functions of z coordinate and O_2/N_2 (%) after **a** pure N_2 and **b** 0.04% O_2/N_2 plasma jet treatment (60 kHz, 50 SLM, 175 W)

plasma jet treatment was obviously wider than that of the pure N_2 one; this shows that the addition of a trace amount of oxygen produced a wider operating window. These results are explained below.

Figures 5 and 6 show the concentrations of O_3 and typical NO-γ UV emission (236.6 nm, photon energy: 5.2 eV), respectively, as a function of downstream distance and O_2/N_2 (%) in the plasma jet region. The resolution distance of the measurement of O_3 concentration distribution and NO-γ UV distribution was 2 mm. The distributions of O_3 show a maximal value at the downstream location of $z \approx 10$ mm for various ratios of O_2/N_2. In addition, the UV emission was very strong in the near jet region (z up to 10 mm), especially when $O_2/N_2 \approx 0.05\%$. It is well known that ozone can effectively absorb UV emissions in the range of 220–280 nm [16]. Thus, an appreciable amount of oxygen radicals $[O_3 + h\upsilon \rightarrow O(^3P) + O_2]$ could be generated in the near jet region ($z < 10$ mm). Note that the NO-γ UV emission was probably caused by the collision of ground NO

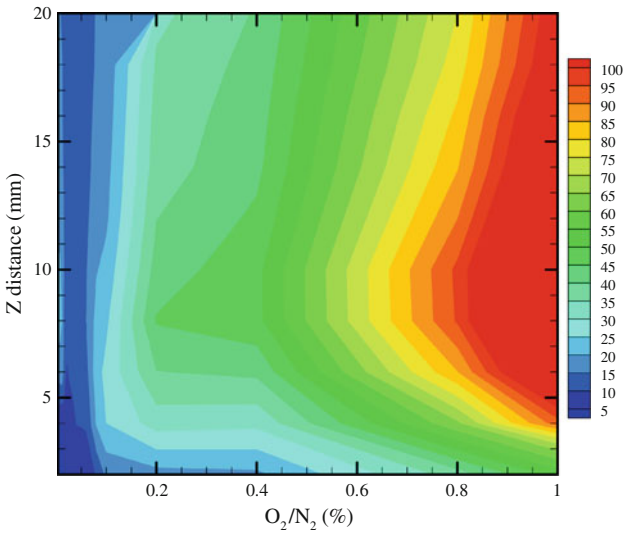

Fig. 5 Distributions of O_3 concentration as functions of downstream distance and O_2/N_2 (%) in post-discharge region (60 kHz, 50 SLM, 175 W)

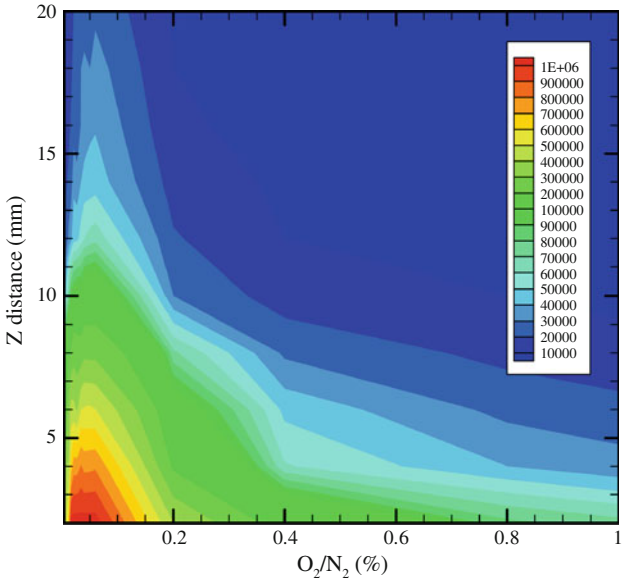

Fig. 6 Distributions of typical NO-γ UV emission intensity (236.6 nm, photon energy: 5.2 eV) as functions of downstream distance and O_2/N_2 (%) in post-discharge region (60 kHz, 50 SLM, 175 W)

species produced in the discharge with the abundant and long-lived metastable N_2 $\left[N_2(A^3\sum_u^+)\right]$ in a nitrogen-based discharge [13]. Higher intensity NO-γ UV emissions did not signify a higher amount of ground NO species since it was also proportional to the amount of metastable N_2, which was strongly dependent on the amount of oxygen addition

and downstream location in the plasma jet. Another possible mechanism for improving the hydrophilic property caused by the existence of metastable N_2 $\left[N_2(A^3\sum_u^+)\right]$ is described next.

Figure 7a, b show the measured optical emission spectra in the range of 180–900 nm in the post-discharge region. In the discharge region, the addition of 0.06% O_2 reduced the production of $N_2(C^3\prod_u)$ $[N_2 + e \rightarrow N_2(C^3\prod_u) + e]$ because of reduced electron number density due to high electron affinity of oxygen. Hence, in the post-discharge region, the emission line intensity for the N_2 2nd positive $\left[N_2(C^3\prod_u) \rightarrow N_2\left(B^3\prod_g\right) + h\upsilon\,(337.1\,nm)\right]$ decreased accordingly (Fig. 7a). However, the addition of 0.06% O_2 increased the amount of ground-state NO and thus $NO(A^2\sum^+)$ and $NO(B^2\prod)$ $\left[NO + N_2\left(A^3\sum_u^+\right) \rightarrow NO(A^2\sum^+)\right.$

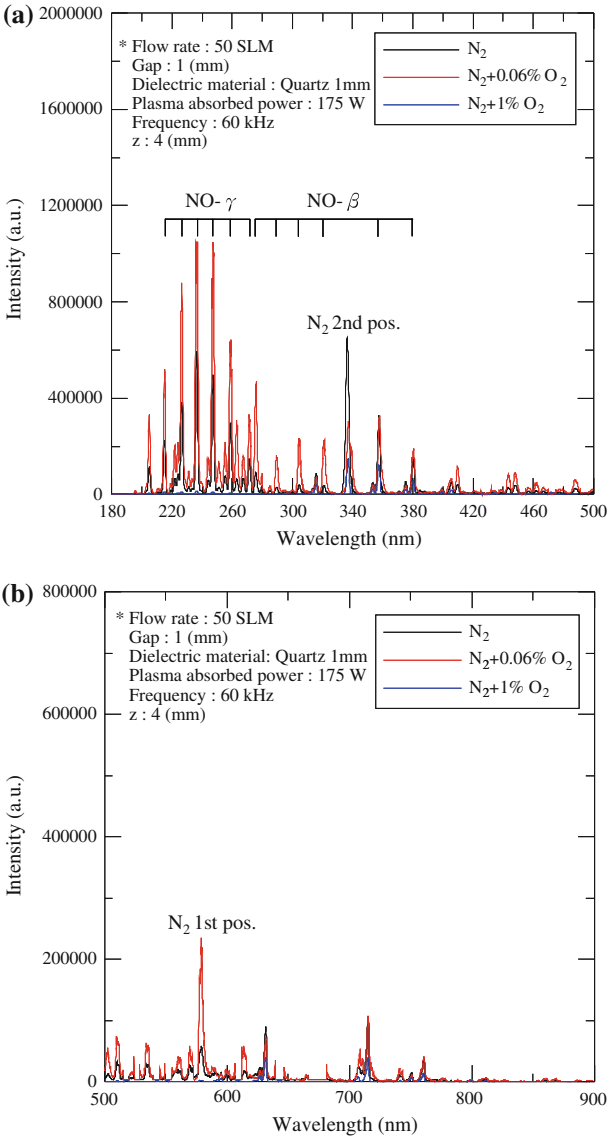

Fig. 7 Optical emission spectrum in the **a** 180–500 nm; **b** 500–900 nm for the post-discharge plasma (60 kHz, 50 SLM, 175 W)

and $NO + N_2(A^3\sum_u^+) \rightarrow NO(B^2\prod)]$. Hence, in the post-discharge region, the NO-γ, the NO-β and the N_2 1st positive (Lewis-Rayleigh afterglow) emission line intensities increased through $[NO(A^2\sum^+) \rightarrow NO + h\upsilon\,(180 - 260nm)]$, $[NO(B^2\prod) \rightarrow NO + h\upsilon\,(260 - 380\,nm)]$ and $[N + N + N_2 \rightarrow N_2(B^3\prod_g)$ and $N_2(B^3\prod_g) \rightarrow N_2(A^3\sum_u^+) + h\upsilon\,(580\,nm)]$, respectively. In the above, the increase of N_2 1st positive line intensity (580 nm) is mainly caused by the increase of N atoms through the reaction channels in the discharge region such as $e + N_2 \rightarrow N_2(a'^1\sum_u^-) + e$ and $N_2(a'^1\sum_u^-) + NO \rightarrow N + O + N_2$ with 0.06% addition of O_2. As more O_2 was added, all line emission intensities decreased because of reduced plasma (thus, electron) intensity in the discharge region [17–21].

These data show that the amount of metastable nitrogen decreased rapidly with the addition of too much oxygen, since oxygen is an electronegative gas which has a very strong electron affinity. However, the quantitative reason for observing the maximal amount of the 1st positive N_2 at $O_2/N_2 = 0.06\%$ is still unknown and deserves further investigation. Note that the metastable N_2 $[N_2(A^3\sum_u^+)]$ energy state is 6.2 eV above the ground state and its lifetime is $\sim$13 s [22]. It is very reactive towards saturated hydrocarbons and can transfer about 6.2 eV efficiently to these molecules to generate dissociative triplet states that break C–H bonds (4.2 eV) and C–C bonds (3.8 eV) [23, 24]. This effect may have been especially important in improving the hydrophilic property of ITO glass at the far downstream locations where the amount of O_2/N_2 was very small (e.g., 0.05–0.06%), and the amount of ozone was also very small (see Fig. 3).

In the first regime (nearly pure nitrogen plasma jet), as indicated in Fig. 3, at the exit of the DBD, the NO-γ UV emission was relatively appreciable (see Fig. 6) since the metastable $N_2(A^3\sum_u^+)$ in the early portion of the plasma jet was still abundant, although the NO concentration would be low under this condition. Note that the residence time of the N_2 $[N_2(A^3\sum_u^+)]$ species for the current test condition was 0.1 ms up to $z = 16$ mm, which was much shorter than its lifetime ($\sim$13 s). Although the amount of NO-γ UV emission decreased rapidly in the downstream direction (because of ambient quenching of the NO and the short-lived excited $N_2(B^3\prod_g)$), the amount of the long-lived metastable $N_2(A^3\sum_u^+)$ was still high enough to transfer energy effectively to break the C–H and C–C bonds of the organic compounds on the ITO glass surface.

In the second regime, as indicated in Fig. 3, at the exit of the DBD, NO-γ UV emission peaked at $\sim$0.05% of oxygen addition and then dropped rapidly due to the quenching of increased oxygen addition (reduced metastable N_2 species), as shown in Fig. 6. In this peak region near the DBD exit, a high intensity of NO-γ UV emission produced better surface cleaning because of more atomic oxygen O produced following the reaction path $(O_3 + h\upsilon \rightarrow O(^3P) + O_2)$, and the abundant metastable N_2 $[N_2(A^3\sum_u^+)]$ transferred energy to break bonds such as C–C (3.8 eV) and C–H (4.2 eV). As more oxygen was added (e.g., 1%), the amount of atomic oxygen decreased accordingly (see Fig. 6) because the NO-γ UV emission was much lower than in the first regime. However, in the further downstream location after $z = 10$ mm, the NO-γ UV emission was reduced to a very small amount, as atomic oxygen O could not be produced effectively; the long-lived N_2 $[N_2(A^3\sum_u^+)]$ then played a key role in surface cleaning, although the CA increased rapidly after this point.

Table 2 summarizes the typical roughness data of stationary ITO glass under various test conditions after surface treatment using the pure N_2 and O_2/N_2 (0.1%) discharge jet with different distances. Note that the RMS roughness data were taken from a 2 μm by 2 μm section. All RMS roughness was in the range of 0.53–0.69 nm, signifying that the application of APPJ did not significantly modify the surface morphology. APPJ only acted

Table 2 RMS Roughness of ITO glass at different treating distances measured by AFM

O_2/N_2 (%)	z (mm)	Speed (cm/s)	Exposure time (s)	Contact angle (°)	RMS roughness (nm)
0	4	0	5	37	0.66
0	10	0	5	20	0.62
0	20	0	5	32	0.63
0	4	9	0.01	73	0.63
0.06	4	0	5	29	0.53
0.06	10	0	5	22	0.53
0.06	20	0	5	54	0.54
0.06	4	9	0.01	42	0.69
Untreated ITO				84	0.68

to remove the attached organic contaminants, which was important for this type of application.

Conclusion

In the current study, a planar DBD APPJ driven by a quasi-pulsed bipolar power supply (60 kHz) was developed and used to clean ITO glass using the post-discharge jet region. Results showed that there existed two distinct regimes having lower CAs in the range of 20–30°. Possible mechanisms of surface cleaning have been presented; they took into account the spatial distribution of O_3, NO-γ UV emission and OES spectra. For ITO cleaning mechanisms, in the near jet downstream location ($z < 10$ mm), both the metastable N_2 $\left[N_2(A^3\sum_u^+)\right]$ and ozone photo-induced dissociation played dominant roles in cleaning ITO glass, although their relative importance was unclear and requires further investigation. In the far jet downstream location ($z > 10$ mm), when the ratio of O_2/N_2 was small, only the long-lived metastable N_2 $\left[N_2(A^3\sum_u^+)\right]$ played a major role in cleaning ITO glass. One final note on using nitrogen as the discharge gas is that nitrogen was easily recycled to a high purity (>99%) using a ceramic membrane [25].

Acknowledgments We would like to thank the National Science Council of Taiwan, the Institute of Nuclear Energy Research of Taiwan and the Ministry of Economic Affairs of Taiwan for their financial support through grants No. 96-2628-E-009-134-MY3, 98I004 and 98-EC-17-A-07-S2-0043 respectively.

References

1. Schütze A, Jeong JY, Babayan SE, Park J, Selwyn GS, Hicks RF (1998) IEEE Trans Plasma Sci 26:1685
2. Chaudhary K, Inomata K, Yoshimoto M, Koinuma H (2003) Mater Lett 57:3046
3. Laroussi M, Akan T (2007) Plasma Proc Polym 4:777
4. Takaki K, Hosokawa M, Sasaki T, Mukaigawa S, Fujiwara T (2005) Appl Phys Lett 86:151501
5. Lee YH, Yeom GY (2005) Jpn J of Appl Phys 44:1076
6. Laroussi M, Leipold F (2004) Int J Mass Spectrom 233:81
7. Meiners S, Salge JGH, Prinz E, Förster F (1998) Surf Coat Technol 98:1121
8. Herrmann HW, Henins I, Park J, Selwyn GS (1999) Phys Plasmas 6:2284
9. Xiong Q, Lu XP, Jiang ZH, Tang ZY, Hu J, Xing ZL, Pan Y (2008) IEEE Trans Plasma Sci 36:986

10. Walsh JL, Shi JJ, Kong MG (2006) Appl Phys Lett 88:171501
11. Jung MH, Choi HS (2007) J of Colloid Interface Sci 310:550
12. Iwasaki M, Takeda K, Ito M, Yara T, Uehara T, Hori M (2007) Jpn J of Appl Phys 46:L540
13. Iwasaki M, Matsudaira Y, Takeda K, Ito M, Miyamoto E, Yara T, Uehara T, Hori M (2008) J Appl Phys 103:023303
14. Wagner HE, Brandenburg R, Kozlov KV, Sonnenfeld A, Michel P, Behnke JF (2003) Vacuum 71:417
15. Yi CH, Jeong CH, Lee YH, Ko YW, Yeom GY (2004) Surf Coat Technol 177–178:711
16. Wameck P (1998) Chemistry of the natural atmosphere. Academic, London
17. Golubovskii YB, Maiorov VA, Behnke J, Behnke JF (2002) J Phys D 35:751
18. Brandenburg R, Maiorov VA, Golubovskii YB, Wagner HE, Behnke J, Behnke JF (2005) J Phys D 38:2187
19. Golubovskii YB, Maiorov VA, Behnke JF, Tepper J, Lindmayer M (2004) J Phys D 37:1346
20. Guerra V, Sá PA, Loureiro J (2001) J Phys D 34:1745
21. Dilecce G, Ambrico PF, Benedictis SD (2007) Plasma Sources Sci Technol 16:511
22. Fridman A, Kennedy LA (2004) Plasma physics and engineering. Taylor and Francis, New York
23. Herron JT (1999) J Phys Chem Ref Data 28:1453
24. Klages CP, Grishin A (2008) Plasma Process Polym 5:368
25. Baker RW (2002) Ind Eng Chem Res 41:1393